

# Phase structure of (2+1)-dimensional compact lattice gauge theories and the transition from Mott insulator to fractionalized insulator

J. Smiseth,\* E. Smørgrav,<sup>1,†</sup> F. S. Nogueira,<sup>2,‡</sup> J. Hove,<sup>1,§</sup> and A. Sudbø<sup>1,\*\*</sup>

<sup>1</sup>*Department of Physics, Norwegian University of Science and Technology, N-7491 Trondheim, Norway*

<sup>2</sup>*Institut für Theoretische Physik, Freie Universität Berlin, D-14195 Berlin, Germany*

(Received 16 January 2003; revised manuscript received 18 March 2003; published 15 May 2003)

Large-scale Monte Carlo simulations are employed to study phase transitions in the three-dimensional compact Abelian Higgs model in adjoint representations of the matter field, labeled by an integer  $q$ , for  $q = 2, 3, 4, 5$ . We also study various limiting cases of the model, such as the  $Z_q$  lattice gauge theory, dual to the three-dimensional (3D) spin model, and the 3D  $XY$  spin model which is dual to the  $Z_q$  lattice gauge theory in the limit  $q \rightarrow \infty$ . In addition, for benchmark purposes, we study the square lattice eight-vertex model, which is exactly solvable and features nonuniversal critical exponents. We have computed the first, second, and third moments of the action to locate the phase transition of the compact Abelian Higgs model in the parameter space  $(\beta, \kappa)$ , where  $\beta$  is the coupling constant of the matter term and  $\kappa$  is the coupling constant of the gauge term. We have found that for  $q=3$ , the three-dimensional compact Abelian Higgs model has a phase-transition line  $\beta_c(\kappa)$  which is first order for  $\kappa$  below a finite *tricritical* value  $\kappa_{\text{tri}}$  and second order above. The  $\beta=\infty$  first order phase transition persists for finite  $\beta$  and joins the second order phase transition at a tricritical point  $(\beta_{\text{tri}}, \kappa_{\text{tri}}) = (1.23 \pm 0.03, 1.73 \pm 0.03)$ . For all other integer  $q \geq 2$  we have considered, the entire phase-transition line  $\beta_c(\kappa)$  is critical. We have used finite-size scaling of the second and third moments of the action to extract critical exponents  $\alpha$  and  $\nu$  without invoking hyperscaling, for the  $XY$  model, the  $Z_2$  spin and lattice gauge models, as well as the compact Abelian Higgs model for  $q=2$  and  $q=3$ . In all cases, we have found that for practical system sizes, the third moment gives scaling of superior quality compared to the second moment. We have also computed the exponent ratio for the  $q=2$  compact  $U(1)$  Higgs model along the critical line, finding a *continuously varying ratio*  $(1+\alpha)/\nu$ , as well as continuously varying  $\alpha$  and  $\nu$  as  $\kappa$  is increased from 0.76 to  $\infty$ , with the Ising universality class  $(1+\alpha)/\nu = 1.763$  as a limiting case for  $\beta \rightarrow \infty, \kappa \rightarrow 0.761$ , and the  $XY$  universality class  $(1+\alpha)/\nu = 1.467$  as a limiting case for  $\beta \rightarrow 0.454, \kappa \rightarrow \infty$ . However, the critical line exhibits a remarkable resilience of  $Z_2$  criticality as  $\beta$  is reduced along the critical line. Thus, the three-dimensional compact Abelian Higgs model for  $q=2$  appears to represent a *fixed-line* theory defining a new universality class. We relate these results to a recent microscopic description of zero-temperature quantum phase transitions within insulating phases of strongly correlated systems in two spatial dimensions, proposing the above to be the universality class of the zero-temperature *quantum phase transition* from a Mott-Hubbard insulator to a charge-fractionalized insulator in two spatial dimensions, which thus is that of the 3D Ising model for a considerable range of parameters.

DOI: 10.1103/PhysRevB.67.205104

PACS number(s): 74.20.-z, 05.10.Cc, 11.25.Hf

## I. INTRODUCTION

Lattice gauge theories in 2+1 dimensions with compact gauge fields coupled to matter fields, have recently come under close scrutiny as effective theories of strongly correlated fermion systems in two spatial dimensions at zero temperature. Phase transitions in such three-dimensional models then correspond to quantum phase transitions in a system at zero temperature in two spatial dimensions. A central issue is whether such systems of strongly correlated fermions can suffer quantum phase transitions from Fermi-liquid metallic states to states where the quasiparticle concept has broken down and given way to singular Fermi liquids<sup>1</sup> or electron-splintered states.<sup>2,3</sup> Such quantum phase transitions may be related to phase transitions such as confinement-deconfinement transitions in (2+1)-dimensional compact gauge theories. This fact has resulted in focused attention on effective gauge theories of matter fields representing charge doped into Mott-Hubbard insulators, coupled to fluctuating gauge fields representing strong constraints on the dynamics of the fermions on the underlying lattice on which the mod-

els are defined.<sup>4-8</sup> Since these are lattice models, the corresponding gauge fields are necessarily compact. Compact  $U(1)$  gauge fields in 2+1 dimensions support stable topological defects in the form of monopole configurations, and it has been suggested that the unbinding of such monopoles, a confinement-deconfinement transition, may be relevant for such phenomena as spin-charge separation in strongly correlated systems.<sup>9,5,8</sup> Confinement here refers to the confinement of test charges in the problem, not of topological defects of the gauge field (which are space-time instantons, and will hereafter be referred to as “monopole” configurations). Alternative formulations in terms of a lattice Ising gauge theory<sup>10</sup> coupled to matter fields, have also been put forth.<sup>11,12,2</sup> This is largely motivated, it would appear, by the fact that it is highly controversial whether a (2+1)-dimensional  $U(1)$  gauge theory with matter fields in the *fundamental representation* will undergo a confinement-deconfinement transition. In the absence of matter fields, compact  $U(1)$  gauge theories are known to be permanently confined in  $d=2+1$ , while the pure  $Z_2$  gauge theory is known to have a second order phase transition in the inverted

3D Ising universality class. It is sometimes stated, without much justification, that the presence of matter fields in the fundamental representation will not alter the picture that emerges in their absence, both for the  $U(1)$  case and the  $Z_2$  case in  $2+1$  dimensions.

One major problem that arises in this context, is that the Wilson loop nonlocal gauge-invariant order parameter, which has proven itself to be very useful in the absence of dynamical matter fields to distinguish confined from deconfined phases, is rendered useless by the presence of them. In particular, when the symmetry group of the matter field is contained in the symmetry group of the gauge field, one can demonstrate rigorously under otherwise quite general conditions, that the Wilson loop is bounded from below by a perimeter law, not an area law, despite the fact that models with this property definitely has phase transitions from confined to deconfined phases.<sup>13</sup> Hence, the Wilson loop and the related Polyakov loop, are no longer useful order parameters for the problem. Physically, this is due to the fact that in the presence of a dynamically fluctuating matter field coupled to the gauge field, particle-hole excitations are generated from the vacuum and will effectively screen the interaction between two static test charges introduced into the system, which the Wilson loop is a measure of. Hence, a perimeter law is always obtained.

Recently, two of us have shown that a confinement-deconfinement transition may take place in three-dimensional compact  $U(1)$  gauge theory coupled to matter fields, when the matter field exhibits *critical* fluctuations.<sup>14,15</sup> Such matter-field fluctuations endow the gauge-field with an anomalous scaling dimension  $\eta_A$  with a value<sup>16,17</sup>

$$\eta_A = 4 - d, \quad (1)$$

where  $d$  is the dimensionality of the system. This value for  $\eta_A$  is protected by gauge invariance. In  $d=3$ , this transforms the gauge-field propagator in a striking manner such as to allow a confinement-deconfinement transition to take place via a three-dimensional Kosterlitz-Thouless like phase transition of unbinding of pointlike monopole configurations of the gauge field.<sup>14,15</sup> The treatment of Refs. 14,15 closely parallels that of Ref. 18 and is based on a dual description in the continuum. However, it is far from obvious what the corresponding *lattice gauge theory*, if any, that would yield such results, could be.

In the absence of a clear-cut order-parameter criterion for distinguishing various phases of such matter-coupled gauge fields, it would be advantageous to be able to distinguish various phases by direct “thermodynamic” measurements reliably exhibiting possible non-analytic behavior. In this paper, we will use one such measurement recently introduced by us,<sup>19</sup> namely, finite-size scaling of the third moment of the action of the lattice model. This will turn out to be a superior quantity to study for this purpose, compared to the second moment. It brings out nonanalytic thermodynamics and precision values of the specific heat critical exponent  $\alpha$  and the correlation length exponent  $\nu$  through finite-size scaling analysis performed on practical system sizes.<sup>19</sup> The third moment has the advantage of not being contaminated by contri-

butions from the second moment. The second moment is known to be a notoriously difficult quantity to use in particular for extracting specific heat exponents, due to large corrections to scaling coming from confluent singularities for practical system sizes. Moreover, the third moment is the simplest quantity to compute which has an extra feature which even moments do not have. It has a double-peak structure where the width *between* the peaks also exhibits scaling. This allows us to extract separately *two* exponents  $\alpha$  and  $\nu$  from measurements of the third moment alone, without having to invoke hyperscaling.

A lattice model of particular interest in this context is the Abelian  $U(1)$  Higgs model with a compact gauge field<sup>18</sup> coupled minimally to a  $U(1)$  bosonic matter field<sup>20,21</sup> with a gauge charge  $q$ . It is defined by the partition function given by the following functional integral

$$Z = \int_{-\pi}^{\pi} \left[ \prod_{j=1}^N \frac{d\theta_j}{2\pi} \right] \int_{-\pi}^{\pi} \left[ \prod_{j,\mu} \frac{dA_{j\mu}}{2\pi} \right] \exp[\beta H_\beta + \kappa H_\kappa],$$

$$H_\beta = \sum_{j,\mu} [1 - \cos(\Theta_{j\mu})],$$

$$H_\kappa = \sum_{P,\mu} [1 - \cos(\mathcal{A}_{j\mu})], \quad (2)$$

where  $N$  is the number of lattice sites and we have defined

$$\Theta_{j\mu} = \Delta_\mu \theta_j - qA_{j\mu},$$

$$A_{j\mu} = \varepsilon_{\mu\nu\lambda} \Delta_\nu A_{j\lambda}. \quad (3)$$

Here,  $\varepsilon_{\mu\nu\lambda}$  is the completely antisymmetric tensor. Moreover,  $\sum_{j,\mu}$  denotes a sum over sites of the lattice, while  $\sum_{P,\mu}$  denotes a sum over the plaquettes of the lattice. We will use the variables ( $x = 1/[\kappa + 1]$ ,  $y = 1/[\beta + 1]$ ) when discussing the possible phases of this model.<sup>20</sup> In Eq. (2),  $\theta$  is the phase of a scalar matter field with unit norm representing holons,  $\Delta_\mu$  is a forward lattice difference operator in direction  $\mu$ , while  $A_{j\mu}$  is the fluctuating gauge field enforcing the onsite constraints reflecting the strong correlations in the problem. We are neglecting amplitude fluctuations of the matter fields, working in the “London limit.”

Let us summarize what is known about this model. When  $q=0$ , the matter field decouples from the gauge field. It is well known that the model then has one critical point in the universality class of the 3D  $XY$  model, and in the Villain approximation (which is most often used when dualizing the model<sup>20</sup>), the critical value  $y_c$  is given by  $y_c \approx 3/4$ .<sup>22,23</sup> On the other hand, the pure gauge theory is permanently confined for all values of  $\kappa$ .<sup>18</sup> Consider next  $q=1$ . Then, Eq. (2) is trivial on the line  $x=1, 0 < y < 1$  with no phase transition for any value of  $y$ . On the line  $0 < x < 1, y=1$  the matter field is absent and the theory is permanently confined.<sup>18</sup> For a further enumeration on rigorous results both on the non-compact and compact version of this model, see also Ref. 24.

For arbitrary  $(\beta, \kappa)$ , the case  $d=3, q=1$  is controversial. It is, however, clear that no ordinary second order phase transition with a local order parameter exists for the model in

this case. When matter fields are coupled to a compact gauge field in a continuum theory, the permanent confinement of the pure gauge theory is destroyed and a confinement-deconfinement transition may take place via a Kosterlitz-Thouless-like unbinding of monopole configurations<sup>14</sup> in three dimensions. This is due to the appearance of an anomalous scaling dimension of the gauge-field induced by critical matter-field fluctuations.<sup>16,17</sup> The role of the anomalous dimension has also been studied recently at finite temperature, in pure compact QED in  $d=3$  with no matter fields present.<sup>25</sup> In both Refs. 14 and 25, the anomalous scaling dimension plays a crucial role. However, in Ref. 25 the deconfinement transition occurs due to finite temperature, and there are no matter fields.

The role of an anomalous scaling dimensions in driving a recombination of monopole defects of the gauge field into dipole configurations, corresponding to a confinement-deconfinement transition, has been studied numerically for the case  $q=1$  in the presence of matter fields.<sup>26</sup> The authors of Ref. 26 in this case reach conclusions in agreement with Ref. 14. Thus, even putting the issue of whether this signals a phase transition or not aside, it is clear that also matter fields in the fundamental representation *do* matter in this problem. It is also interesting to note in this context, that some time ago a rather remarkable paper,<sup>27</sup> a Kosterlitz-Thouless transition was claimed in a three-dimensional theory of integer point charges interacting via a logarithmic potential. There, however, the origin of the logarithmic interaction was due to higher order anisotropic gradient terms, essentially an input to the theory, and not a *result* of an anomalous scaling dimension appearing due to criticality in the mass-sector of a compact  $U(1)$  gauge theory. This, however, contrasts with the case considered in Ref. 14. The anisotropy effectively leads to a dimensional reduction and a resulting standard Kosterlitz-Thouless phase transition in two dimensions.

For  $q>1$  the model in Eq. (2) exhibits a behavior that completely sets it apart from the case  $q=1$ . The reason is that for  $q>1$ , the matter field is no longer in the fundamental representation. Thus, in contrast to the no-compact case of the standard Maxwell term of the gauge sector, the gauge charge cannot be simply scaled away. The case  $q=2$  is particularly interesting in the context of electron fractionalization.<sup>28</sup> This is a case that we will consider in detail in this paper. This theory arises as a special limit of a bosonic model exhibiting fractionalized phases considered recently.<sup>28</sup> The phase diagram for  $q=2$  was briefly discussed long ago by Fradkin and Shenker.<sup>21</sup> For  $d=3$  the phase diagram is divided into two phases, a confined and a deconfined-Higgs phase. There is no Coulomb phase in three dimensions. The model becomes a  $Z_2$  gauge theory on the line  $y=0$ . This limit suffices to bring out the fundamental difference between the  $q=1$  and  $q=2$  cases, since on the line  $y=0$ , the  $q=1$  case is trivial. We will discuss this in more detail below. The vortex content of the  $q=2$  case is different:  $Z_2$  vortices, or *visons*, may arise in the deconfined-Higgs phase. Due to the visons the flux is quantized in units of  $2\pi$  instead of  $\pi$ . This means that the excitations in the deconfined-Higgs phase have charge  $e/2$ . In the context of

the bosonic model in Ref. 28, this phase corresponds to a fractionalized insulator. The confined phase, on the other hand, features excitations with charge  $e$  and should correspond to a conventional Mott insulator.<sup>28</sup> Thus, the model (2) can be thought as describing a particular case of insulator-fractionalized insulator transition. The full bosonic model considered in Ref. 28 has a more rich phase structure depending on the values of the parameters. For example, a superfluid phase is also possible. We will not consider such a situation here, but only a special limit of the bosonic model of Ref. 28.

The purpose of this paper is to make a detailed numerical study of the phase structure of Eq. (2). An important point concerns the universality class of the phase transition. This will be the main topic discussed in this paper. We have performed a large scale Monte Carlo study which gives a very complete picture of the universality class of the transition. The present study complements and goes far beyond our previous large scale Monte Carlo study of the model.<sup>19</sup> In Ref. 19, we have shown that the Ising ( $Z_2$ ) universality class dominates over a significant portion of the critical line of the theory. Moreover, we have shown that there is a region of parameters where the critical exponents are continuously varying. This was interpreted as evidence for the existence of a line of fixed points in the renormalization group (RG) flow diagram. To the portions of the critical line corresponding respectively to  $Z_2$  and  $XY$  critical behavior, are associated Ising and  $XY$  fixed points. In addition to these two fixed points there exists a fixed line corresponding to a critical phase. As discussed recently,<sup>3</sup> electron fractionalization in  $1+1$  dimensions is associated to a quantum critical phase. Ordinarily, in more than one spatial dimension quantum phase transitions are associated with a critical point. Thus, we would expect that electron fractionalization would occur at a critical point. Our analysis clearly shows that a critical phase exists for the model (2) at  $q=2$ . This becomes particularly clear on the portion of the critical line corresponding to large values of  $\kappa$ , where we find that the critical exponents vary smoothly with coupling constants, approaching the 3D  $XY$  value only slowly. The three-dimensional KT-like scenario<sup>14,15</sup> for the  $q=1$  model is also an example of critical phase occurring in higher dimensions. However, due to the vortex content of the model at  $q=1$ , it is not entirely obvious that the corresponding deconfinement transition is really associated with electron fractionalization.<sup>29</sup>

In this paper the cases  $q=3, 4$ , and  $5$  will also be considered. The case  $q=3$  is particularly interesting. While for  $q=2, 4$ , and  $5$  the *entire* line separating the two phases are critical, this is not true when  $q=3$ . In this case there is a value of  $\kappa$  below which the transition is first order, being second order otherwise. This point where the transition changes from second order to first order, is clearly a tricritical point. We emphasize that among the situations analyzed in this paper, only the case  $q=3$  exhibits a tricritical point. When  $q=3$ , charge is fractionalized in such a way that excitations carry charge  $e/3$ . This situation is reminiscent of the  $\nu=1/3$  state in the fractional quantum Hall effect.<sup>30</sup> In general the charge for arbitrary  $q$  will fractionalize as  $e/q$ . This gives an elementary flux quantum  $\phi_0=2\pi q/e$ , contrasting

with the more familiar situation of flux quantization in a superconductor. Indeed, if we take the example of the  $q=2$  theory, we see that the flux quantum is doubled, while in a superconductor it is halved because the Cooper pair has charge  $2e$ . Other interesting possibilities of vortex/charge fractionalization were considered recently in certain Josephson junction arrays.<sup>31</sup>

In all these examples, it is readily seen that the type of flux quantization involved depends on specifying whether charge is fractionalized or not. Therefore, in order to detect charge fractionalization, experimental measurements of flux as the one proposed in Ref. 32 in the context of underdoped cuprates are important. The experiment proposed in Ref. 32 has now been performed,<sup>33</sup> but has failed in detecting electron fractionalization. The failure of this experiment does not, however, entirely rule out charge fractionalization in the cuprates for the following deep reason. In the zero doping insulating regime, the system can effectively be described by the antiferromagnetic quantum Heisenberg model. This model is known to have a local  $SU(2)$  gauge symmetry.<sup>34</sup> Upon doping, this symmetry is broken down to  $U(1)$ . Since this  $U(1)$  is a subgroup of  $SU(2)$ , it is compact and carries the “charge” label  $q$  corresponding to the different representations. Within the  $q=2$  representation, the double broken symmetry pattern  $SU(2) \rightarrow U(1) \rightarrow Z_2$  is possible. In such a situation, there would be no stable vison and any experimental attempt based on a vison trapping experiment would fail. However, this does not mean that charge is not fractionalized. The  $Z_2$  residual subgroup will imply the existence of magnetic monopoles which, by duality, accounts for the existence of fractional charges  $e/2$ . In the perspective of such a possible scenario, alternative experimental proposals should be envisioned and the identification of the universality class of possible phase transitions the  $q=2$  case is important in this context.

The plan of the paper is the following. In Sec. II, we discuss the limits of the model, pointing out the differences with respect to the  $q=1$  case. In Sec. III, we explain the finite-size scaling analysis of the third moment of the free energy used in this paper. In Sec. IV we discuss the details of our large-scale Monte Carlo simulations. As a check on the quality of the simulations, we have performed several benchmark simulations which we present in parallel with our new results on the model defined by Eq. (2). Section V concludes the paper.

## II. LIMITS OF THE COMPACT GAUGE THEORY

### A. $\beta \rightarrow \infty$ , $\kappa$ finite

In terms of the formulation of the model in Eq. (2), this limit leads to the constraint  $\Delta_\mu \theta_j - q A_{j\mu} = 2\pi l_{i,\mu}$  where  $l_{i,\mu}$  is integer valued. Substituting this into the gauge-field term, we find

$$Z = \prod_{j=1}^N \sum_{l_{j,\mu}=-\infty}^{\infty} \exp \left\{ \kappa \sum_{P,\mu} \left[ 1 - \cos \left( \frac{2\pi}{q} \mathcal{L}_{j,\mu} \right) \right] \right\}, \quad (4)$$

where  $\mathcal{L}_{j,\mu} = \varepsilon_{\mu\nu\lambda} \Delta_\nu J_{j,\lambda}$  is also integer valued. For  $q=1$  the model is therefore trivial in this particular limit, in accor-

dance with the discussion in the previous section. For  $q=2$ , the model is equivalent to the lattice  $Z_2$  gauge theory,<sup>10</sup> and the critical point of the model in this limit is thus in the inverted Ising universality class (in analogy with the inverted  $XY$  universality class of the dualized 3D  $XY$  model<sup>35</sup>). Therefore  $\alpha$  and  $\nu$  are those of the global 3D Ising model. For integer  $q \geq 3$ , the critical exponents  $\alpha$  and  $\nu$  we will find in the limit  $\beta \rightarrow \infty$ ,  $\kappa$  fixed, will be those of the  $Z_q$  spin model, since as we shall see below, the  $Z_q$  gauge theory is dual to the  $Z_q$  spin model in  $d=3$ .

For arbitrary integer-valued gauge charge  $q$  (i.e., labeling of matter-field representation where  $q=1$  means fundamental representation, while  $q \geq 2$  means higher representations), we may write the action in Eq. (2) in the Villain approximation, replacing the cosine terms by periodic quadratic parts, after which the model may be written in terms of its topological defects as<sup>20,8</sup>

$$Z = Z_0 \sum_{\{Q_j\}} \sum_{\{J_{j\nu}\}} \delta_{\Delta_\nu J_{j\nu}, q Q_j} \exp \left[ -4\pi^2 \beta \times \sum_{j,k} \left( J_{j\nu} J_{k\nu} + \frac{q^2}{m^2} Q_j Q_k \right) D(j-k, m^2) \right], \quad (5)$$

where  $D(j-k, m^2) = (-\Delta_\lambda^2 + m^2)^{-1} \delta_{jk}$  and  $m^2 = q^2 \beta / \kappa$ . Here  $Z_0$  is the partition function for massive spin waves,<sup>20</sup> and is an analytic function of coupling constants which will be omitted from now on. Note the appearance of the constraint

$$\Delta_\nu J_{j\nu} = q Q_j; \quad q \in \mathbb{N} \quad (6)$$

in the summation, which will be important in what follows. Here,  $Q_j \in \mathbb{Z}$  is the monopole charge on (dual) lattice site number  $j$ , while  $J_{j\nu}$  are topological currents representing segments of open-ended strings terminating on monopoles, or closed loops. These are the only stable topological objects of the theory.<sup>20</sup> For a recent treatment of the interplay between Abelian monopole condensation and vortex condensation in lattice gauge theories, see Ref. 36.

In the limit  $\beta \rightarrow \infty$  at fixed  $\kappa$ , the partition function in Eq. (5) takes the form

$$Z = \sum_{\{Q_j\}} \sum_{\{J_{j\nu}\}} \delta_{\Delta_\nu J_{j\nu}, q Q_j} \exp \left( -\frac{2\pi^2 \kappa}{q^2} \sum_j J_{j\nu}^2 \right). \quad (7)$$

This is easily seen to be the loop-gas representation of the global  $Z_q$  theory in the Villain approximation.<sup>37</sup> Using the integral representation of the Kronecker delta and summing over  $J_{j\nu}$  using the Poisson formula, we obtain up to an overall nonsingular factor

$$Z = \sum_{\{N_{j\nu}\}} \int_{-\pi}^{\pi} \left[ \prod_{j=1}^N \frac{d\theta_j}{2\pi} \right] \times \exp \left[ -\frac{q^2}{8\pi^2 \kappa} \sum_{j,\nu} (\Delta_\nu \theta_j - 2\pi N_{j\nu})^2 + i q \sum_j Q_j \theta_j \right]. \quad (8)$$

By employing the Poisson identity

$$\sum_{Q=-\infty}^{\infty} e^{iqQ\theta} = 2\pi \sum_{l=-\infty}^{\infty} \delta(\theta - 2\pi l/q), \quad (9)$$

we obtain

$$Z = \sum_{\{l_j = -q+1\}}^{q-1} \sum_{\{N_{j\nu}\}} \exp \left[ -\frac{q^2}{8\pi^2\kappa} \sum_{j,\nu} \left( \frac{2\pi}{q} \Delta_{\nu} l_j - 2\pi N_{j\nu} \right)^2 \right]. \quad (10)$$

The above is precisely the Villain form of a  $Z_q$  model.<sup>37</sup>

Since Eqs. (7) and (4) are dual (up to a Villain approximation), and Eq. (7) is a loop-gas representation of the global  $Z_q$  theory while Eq. (4) is the  $Z_q$  lattice gauge theory, we conclude that the global and local  $Z_q$  theories are dual to each other in  $d=3$ , in agreement with the results of Ref. 38. Hence, again we conclude that the model Eq. (2) in the limit  $\beta \rightarrow \infty$ ,  $\kappa$  fixed, should have critical exponents  $\alpha$  and  $\nu$  consistent with the  $q$ -state clock model universality class. Since  $\lim_{q \rightarrow \infty} Z_q = U(1)$ , the above fits nicely in with what is known for the  $U(1)$  case in  $d=3$ , where the global 3D  $XY$  model dualizes into a  $U(1)$  gauge theory.<sup>35,39-41</sup>

From Eq. (7), it is seen that the cases  $q=1$  and  $q \neq 1$  are fundamentally different. For  $q=1$ , the summations over  $\{Q_i\}$  may be performed to produce a unit factor at each of the  $N$  dual lattice site, thus completely eliminating the constraint.<sup>23</sup> Hence, we have  $Z = [\vartheta_3(0, e^{-2\pi^2\kappa})]^N$  where the elliptic Jacobi functions are given by  $\vartheta_3(z, q) = \sum_{n=-\infty}^{\infty} q^{n^2} \exp(2\pi i n z)$ , which are analytic functions and hence no phase transition occurs at any value of  $\kappa$  for  $q=1$  in this limit. For (integer)  $q \geq 2$ , a phase transition is known to survive.<sup>21</sup> The restoration of a phase transition for integer  $q > 1$  is, in this language, crucially dependent on the presence of the constraint Eq. (6) for  $q \neq 1$ . Even when one sums over *all* possible values of  $\{Q_j\}$ , this still represents a real constraint on the vortex configurations of the system, since it cannot be eliminated by summation as in the case of  $q=1$ . This suffices to convert the theory to a strongly interacting one capable of sustaining a phase transition, in contrast to the effectively (discrete Gaussian) noninteracting case  $q=1$ .

### B. $\beta$ finite, $\kappa \rightarrow \infty$

We now discuss the limit  $\beta$  finite,  $\kappa \rightarrow \infty$ . Note from Eq. (2), that when  $\kappa \rightarrow \infty$ , we have  $\varepsilon_{\mu\nu\lambda} \Delta_{\nu} A_{j\lambda} = 2\pi M_{j,\mu}$ , where  $M_{j,\mu}$  is integer valued. This shows that in this limit, the gauge-field fluctuations are very similar to transverse phase fluctuations in the 3D  $XY$  model,<sup>42</sup> and the integer  $M_{j,\mu}$  plays the role of vorticity. Thus, even when  $\kappa \rightarrow \infty$ , gauge-field fluctuations are not completely suppressed, we are not allowed to set  $M_{j,\mu} = 0$ , and hence we cannot set  $A_{j,\mu} = \Delta_{\mu} \chi_j$  in the first term in Eq. (2). However, we may write the partition function on the form

$$Z = \int_{-\pi}^{\pi} \left[ \prod_{j=1}^N \frac{d\theta_j}{2\pi} \right] \int_{-\pi}^{\pi} \left[ \prod_{j,\mu} \frac{dA_{j\mu}}{2\pi} \right] \exp[\beta H_{\Theta}], \quad (11)$$

where the functional integral over the gauge field is now constrained. Introducing the Villain approximation, using the

Poisson summation formula, integrating over  $\theta_j$ , and performing a partial integration, leads to the partition function which is equivalent to an ordinary loop gas with completely suppressed gauge-field fluctuations when  $q$  is an integer. The gauge-field fluctuations of the compact sector produce closed vortex loops with long-range interactions such that the loop tangle is incompressible, entirely equivalent to ordinary matter field vortex loops. No screening of their test charges is produced by these constrained gauge-field fluctuations and monopole configurations are suppressed. Hence, the model in this limit is, after all, equivalent to the 3D  $XY$  model, as it also is in the noncompact case where gauge-field fluctuations are entirely suppressed.

Ideally, to explore the entire phase diagram of the model Eq. (2), we could carry out Monte Carlo (MC) simulations in conjunction with finite-size scaling analysis of standard quantities such as the susceptibility or the specific heat. The problem with the former quantity is that we have no candidate gauge-invariant order parameter for this model, in view of the results of Refs. 13,43,44. The problem with the latter is that the second moment of the action is marred with huge corrections to scaling and is hence unsuitable to extract critical exponents from simulations on practical system sizes. To circumvent this difficulty, we will consider various higher order *moments* of the action appearing in the partition function in order to obtain quantities with good scaling for practical system sizes we can handle in Monte Carlo simulations.

### III. MOMENTS OF THE ACTION

Given a singular contribution to the free energy  $F = -\ln Z$  of a system with an inverse temperature coupling  $\beta$ ,

$$F_{\text{sing}} \sim |t|^{2-\alpha} \mathcal{F}_{\pm}(h/|t|^{\Delta}), \quad (12)$$

where  $h$  plays the role of a scaling variable,  $\Delta$  is some scaling exponent,  $\lim_{x \rightarrow \infty} \mathcal{F}_{\pm}(x) \sim x^{(2-\alpha)/\Delta}$ ,  $\lim_{x \rightarrow 0} \mathcal{F}_{\pm}(x) = A_{\pm}^{\mathcal{F}}$ ,  $A_{\pm}^{\mathcal{F}}$  are critical amplitudes, and  $t = (\beta - \beta_c)/\beta$  is some deviation from a critical coupling, then the nonanalytic contribution to the susceptibility of the action is given by

$$C \sim |t|^{-\alpha} C_{\pm}(h/|t|^{\Delta}), \quad (13)$$

where  $\lim_{x \rightarrow \infty} C_{\pm}(x) \sim x^{-\alpha/\Delta}$ , and  $\lim_{x \rightarrow 0} C_{\pm}(x) = A_{\pm}^C$ . At a critical point, this quantity will scale as  $C \sim L^{\alpha/\nu}$ , where the volume of the system is given by  $L \times L \times L$ , provided the system exhibits one diverging length scale at the phase transition. Here,  $\nu$  is the correlation length critical exponent,  $\xi \sim |t|^{-\nu}$  close to a critical point. A problem arises if  $\alpha < 0$ , as in the 3D  $XY$  model, since one then gets an increasing peak in  $C$  itself with increasing  $L$ , which, however, eventually will no longer scale with  $L$ . Unfortunately, but quite typically, impractically large system sizes are needed to eventually distinguish corrections to scaling from actual scaling in the second moment, particularly so when  $\alpha < 0$ . Thus,  $C$  exhibits a finite cusp nonanalyticity which does scale, superposed on a large regular background which eventually will not. It would be advantageous to be able to subtract out this background, or at the very least bring out the leading non-analyticity dominating the scaling more clearly relative to confluent sin-

gularities, or corrections to scaling. This can effectively be achieved by taking one further derivative of the action with respect to the coupling constant as

$$\frac{\partial^3 F_{\text{sing}}}{\partial \beta^3} \sim |t|^{-(1+\alpha)} \mathcal{G}_{\pm}(h/|t|^{\Delta}), \quad (14)$$

where the scaling function  $\mathcal{G}_{\pm}(x)$  has the properties  $\lim_{x \rightarrow \infty} \mathcal{G}_{\pm}(x) \sim x^{-(1+\alpha)/\Delta}$  and  $\lim_{x \rightarrow 0} \mathcal{G}_{\pm}(x) \rightarrow A_{\pm}^{\mathcal{G}}$ , which will scale as  $L^{(1+\alpha)/\nu}$  at a critical point.

More generally, the  $n$ th moment

$$\frac{\partial^n F_{\text{sing}}}{\partial \beta^n} \sim |t|^{-(n-2+\alpha)} \mathcal{G}_{\pm}(h/|t|^{\Delta}), \quad (15)$$

will scale as  $L^{(n-2+\alpha)/\nu}$  at a critical point, and therefore by computing two moments, say the third ( $n=3$ ) and the fourth ( $n=4$ ), it is also possible to extract  $\alpha$  and  $\nu$  separately without utilizing the hyperscaling relation  $\alpha=2-d\nu$ .

In fact, this may be obtained from the third moment  $M_3$  alone, since the width between the negative and positive peaks scales as  $L^{-1/\nu}$ . Thus  $M_3$  yields independent measurements of both  $(1+\alpha)/\nu$  and  $1/\nu$ . The above procedures may serve as *checks* on the validity of hyperscaling. This is known to be violated above the upper critical dimension in spin models and systems with long-range interactions due to the presence of dangerous irrelevant variables.<sup>45</sup> Long-range interactions are features of the *dual* models of some of the theories we consider and little is known about the presence of dangerous irrelevant operators in some of the models we study in this paper. Hence, caution is necessary in extracting individual exponents. At any rate, the above seems to be a useful way of extracting two exponents  $\alpha, \nu$  from measurements of one quantity, namely,  $M_3$ . The procedure described above will presumably turn out to be useful in a host of other models in statistical physics.

Consider next a model with two coupling constants  $x_1$  and  $x_2$  defined by its action

$$S = x_1 H_1 + x_2 H_2. \quad (16)$$

In this case, the scaling of  $\partial^2 F / \partial x_i \partial x_j$  could conceivably depend on the direction in parameter space in which the critical line is crossed. To take this complication into account, we consider contributions to the free energy to second order in deviations in the coupling constants from their critical values, by expanding to second order around the critical point

$$F = -\ln Z = F(\{x_c\}) + \frac{1}{2} \sum_{i,j} \delta x_i \delta x_j \left. \frac{\partial^2 F}{\partial x_i \partial x_j} \right|_{\{x_c\}} + \mathcal{O}(\delta x_i^3).$$

This contribution to the free energy can be written  $\tilde{\delta}x^T F_{ij} \tilde{\delta}x \equiv F^{(2)}$ , where  $F_{ij}$  is the ‘‘fluctuation matrix’’ defined by

$$F_{ij} \equiv \langle H_i H_j \rangle - \langle H_i \rangle \langle H_j \rangle = \frac{\partial^2 F}{\partial x_i \partial x_j}. \quad (17)$$

This can be diagonalized via an orthogonal transformation by rotating the original coupling constant basis through an

angle  $\theta$ ,<sup>46</sup> providing a new set of coordinates which are linear combinations of coupling constants

$$\begin{aligned} x'_1 &\equiv x_1 \cos \theta + x_2 \sin \theta, \\ x'_2 &\equiv -x_1 \sin \theta + x_2 \cos \theta, \end{aligned} \quad (18)$$

with the corresponding uncorrelated operators

$$\begin{aligned} H'_1 &\equiv H_1 \cos \theta + H_2 \sin \theta, \\ H'_2 &\equiv -H_1 \sin \theta + H_2 \cos \theta. \end{aligned} \quad (19)$$

This yields

$$\begin{aligned} F^{(2)} &= (\delta x'_1, \delta x'_2) \begin{pmatrix} \lambda_+ & 0 \\ 0 & \lambda_- \end{pmatrix} \begin{pmatrix} \delta x'_1 \\ \delta x'_2 \end{pmatrix} \\ &= (\delta x'_1)^2 \lambda_+ + (\delta x'_2)^2 \lambda_-, \end{aligned} \quad (20)$$

where  $\lambda_+$  and  $\lambda_-$  are the larger and smaller eigenvalue, respectively. If  $\lambda_+ \gg \lambda_-$  the first term will dominate the leading order corrections to  $F(\{x_c\})$ . Hence, to obtain proper scaling, the second derivative of the free energy should be evaluated along the direction of the corresponding eigenvector

$$\frac{\partial^2 F}{\partial x_1'^2} \sim |x'_1 - x'_{1c}|^{-\alpha}, \quad (21)$$

when crossing the critical line.

From Eq. (2), we get the standard expressions

$$\begin{aligned} \frac{\partial F}{\partial \mu} &= -\langle H_{\mu} \rangle, \\ \frac{\partial^2 F}{\partial \mu^2} &= \langle G_{\mu}^2 \rangle, \end{aligned} \quad (22)$$

where  $\mu$  is the rotated coordinate along the eigenvector corresponding to the largest eigenvalue, and where we have defined  $G_{\mu} = H_{\mu} - \langle H_{\mu} \rangle$  with rotated operator  $H_{\mu}$  defined by Eq. (19). The above expressions essentially represent generalizations of the expressions for internal energy and specific heat. The second derivative contributes to  $C_{\mu}$  which we will refer to as the singular part of the second moment of the action, or the action susceptibility. Similarly, we obtain

$$\frac{\partial^3 F}{\partial \mu^3} = \langle G_{\mu}^3 \rangle, \quad (23)$$

and in general we have for the  $n$ th moment

$$\frac{\partial^n F}{\partial \mu^n} = \langle G_{\mu}^n \rangle. \quad (24)$$

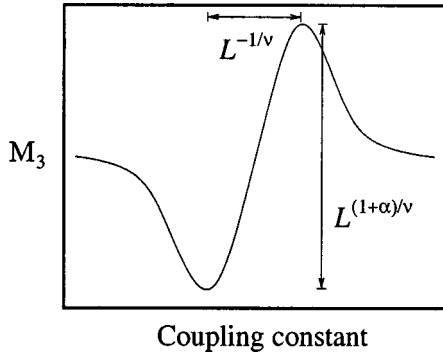


FIG. 1. Generic third moment of action  $M_3$  showing how finite-size scaling is used to extract  $\alpha$  and  $\nu$ .

#### IV. MONTE CARLO SIMULATIONS

##### A. Details of the MC simulations

The critical properties of the models are investigated using large scale Monte Carlo simulations in conjunction with finite-size scaling analysis. A Monte Carlo move is an attempt to replace the field value at one particular point by a randomly chosen value. The move is rejected or accepted according to the standard Metropolis algorithm. In the case of the  $XY$  model, the phase  $\theta_j$  is the relevant field, whereas in the full Abelian Higgs model both the phase and the three components of the gauge field  $A_{j,\mu}$  are subjected to the Metropolis algorithm. One sweep consists of traversing the system  $L \times L \times L$  while attempting a Metropolis update of each field component once. The acceptance rate of the Metropolis algorithm is kept fixed between 60 and 70% by dynamically adjusting the maximum allowed changes in the fields. However, for the model defined in Eq. (2) at large  $\beta$ , where  $Z_q$  gauge behavior is expected, the algorithm for controlling the acceptance rate has been relaxed by fixing the maximum allowed change to  $2\pi$ . There is no gauge fixing involved in these simulations, and periodic boundary conditions are used in all directions. The excess gauge volume due to the summation in the partition function over (redundant) gauge-equivalent field configurations, will cancel out when computing all averages of gauge-invariant quantities, in particular when computing moments of the gauge-invariant action.

The third moment of the action will typically behave as shown in Fig. 1. The MC simulations for the compact Abelian Higgs model will be performed for a set of coupling constants that span a line across the phase transition. We diagonalize the “fluctuation” matrix (17) and simulate along the trajectory  $\beta(\kappa) = \beta_c + a(\kappa - \kappa_c)$ , with  $a$  being determined from the eigenvector with the largest eigenvalue. In all models that we consider in this paper, including benchmark models, we then compute the moments of the action according to Eq. (24) applying Ferrenberg-Swendsen multi-histogram reweighting analysis with jackknifing error estimate. For the benchmark models, this procedure produces curves as shown in Figs. 3 and 4. The top and bottom values as well as their positions for different system sizes are then used to produce scaling plots as shown in Fig. 5. The combinations of critical exponents  $(1 + \alpha)/\nu$  and  $1/\nu$  are then extracted by bootstrap regression analysis.

##### B. Simulations of the eight-vertex model

As a first benchmark on our method of extracting the exponents  $\nu$  and  $\alpha$  separately, we consider the eight-vertex model<sup>47</sup> on a square lattice. This model has the virtue of being exactly solvable, and hence an analytic expression for the exponent  $\nu$  is known. Moreover, it has critical exponents that are nonuniversal.<sup>47</sup> The eight-vertex model on a square lattice may be formulated as a generalized Ising model as<sup>47</sup>

$$Z_{8V} = \sum_{\{\sigma_i\}} \exp[\beta H_{8V}],$$

$$H_{8V} = J_1 \sum_{\langle\langle i,j \rangle\rangle} \sigma_i \sigma_j + J_2 \sum_P \sigma_i \sigma_j \sigma_k \sigma_l, \quad (25)$$

where  $\sigma_i = \pm 1$ ,  $\langle\langle i,j \rangle\rangle$  denotes a summation over nearest neighbors (diagonal bonds) and  $\sum_P$  denotes a sum over the elementary plaquettes on the square lattice. In the above, we have specialized to the case where spin couplings along horizontal and vertical bonds have been omitted. The critical temperature and  $\nu$  are given by

$$e^{-2\beta_c J_2} = \sinh(2\beta_c J_1),$$

$$\frac{1}{\nu} = 2 - \frac{2}{\pi} \cos^{-1}[\tanh(2\beta_c J_2)]. \quad (26)$$

We have computed  $M_3$  for this model, using system sizes  $L \times L$ , with  $L = 8, 12, 20, 40, 60, 80, 120, 200$ . We have used the Metropolis algorithm with single-spin updates, and up to  $5.0 \times 10^5$  sweeps over the lattice for each coupling constant. From this, we have extracted scaling plots of the peak heights and width between peaks of  $M_3$  as a function of system size. From this, we directly extract the combinations  $1/\nu$  and  $(1 + \alpha)/\nu$ , the final results for the exponents are given in Fig. 2. The agreement between our simulation results and the analytical result Eq. (26) is excellent. The above demonstrates that for this model, the third order moment provides an excellent means of extracting nonuniversal exponents from practically accessible system sizes, and in our view provides a first excellent and highly nontrivial benchmark test on the method. We next provide further benchmark tests on a number of 3D systems, before going on to extracting exponents for the (2+1)-dimensional compact Abelian Higgs model.

##### C. Simulations of the 3D $XY$ -, Ising-, and Ising ( $Z_2$ ) gauge models

We reemphasize that what follows in this section is a benchmark on the method of bringing out nonanalytic thermodynamics without recourse to order parameter measurements, by measuring third moments of the action. In later sections the method will be applied to a lattice gauge model for which no nonlocal order parameter currently is known, and where we will obtain precise values of critical exponents. In the present section, we will reproduce known results for the critical exponents  $\alpha$  and  $\nu$  for the 3D  $XY$  model, and the two 3D Ising models, directly from third moments of

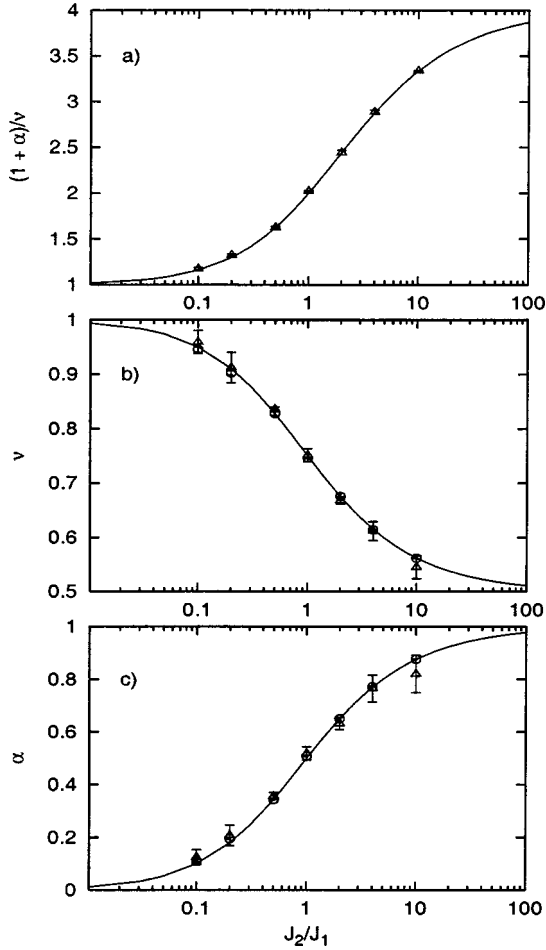


FIG. 2. (a)  $(1 + \alpha)/\nu$  from FSS finite-size of  $M_3$  for Eq. (25) as a function of  $J_2/J_1$ . (b) Same for the exponent  $\nu$ , computed directly from  $M_3$  ( $\Delta$ ) and combining results for  $(1 + \alpha)/\nu$  with hyperscaling ( $\circ$ ). (c)  $\alpha$  as computed directly from  $M_3$  ( $\Delta$ ) and using results for  $(1 + \alpha)/\nu$  with hyperscaling ( $\circ$ ). The solid line in (b) represent the analytical result Eq. (26). The solid lines in (a) and (c) are obtained from Eq. (26) and using hyperscaling  $\alpha = 2 - 2\nu$ . The above results thus also provide a check on hyperscaling in this model.

the action, thus benchmarking the method. We will demonstrate that the method of using the third moment of the action is far superior to using the second moment, for practical system sizes accessible in numerical simulations. This is due to the fact that the third moment is not contaminated by contributions from the second moment, which unfortunately often is marred by contributions from confluent, or subdominant, singularities.

The  $XY$  and Ising models are defined by the following two partition functions

$$Z_{XY} = \int_{-\pi}^{\pi} \left[ \prod_{j=1}^N \frac{d\theta_j}{2\pi} \right] \exp(\beta H_{XY}),$$

$$H_{XY} = \sum_{j,\mu} \cos(\Delta_{\mu} \theta_j),$$

$$Z_I = \sum_{\{\sigma_i = \pm 1\}} \exp(\beta H_I),$$

$$H_I = \sum_{\langle i,j \rangle} \sigma_i \sigma_j.$$

In addition, we consider the three-dimensional Ising lattice gauge theory<sup>10</sup>

$$Z_{\text{IGT}} = \sum_{\{U_{ij} = \pm 1\}} \exp(\beta H_{\text{IGT}}),$$

$$H_{\text{IGT}} = \sum_P U_{ij} U_{jl} U_{lk} U_{ki},$$

where the summation in the last expression runs over all plaquettes  $P$  of the lattice. We note for later use that the Ising model ( $Z_2$  spin model) defined by  $Z_I$  and the Ising gauge theory ( $Z_2$  gauge theory) defined by  $Z_{\text{IGT}}$  are dual to each other in  $d=3$ .<sup>37</sup>

The second and third moments  $M_2$  and  $M_3$  we will consider for these models are given by

$$M_2 = \frac{\partial^2 F}{\partial \beta^2} = \langle G_{\lambda}^2 \rangle,$$

$$M_3 = \frac{\partial^3 F}{\partial \beta^3} = \langle G_{\lambda}^3 \rangle, \quad (27)$$

where  $\lambda \in (XY, I, \text{IGT})$  and where  $I$  and  $\text{IGT}$  denote the Ising and Ising gauge theories, respectively. In all these cases, scaling  $\sim L^{\alpha/\nu}$  is expected for the peak in the second moment, while scaling  $\sim L^{(1+\alpha)/\nu}$  and  $\sim L^{-1/\nu}$  is expected for the third moment peak-to-peak height and width, respectively, as indicated in Fig. 1. We mention in passing that for the 3D  $XY$  model, we have  $(1 + \alpha)/\nu = 1.467$ , while  $(1 + \alpha)/\nu = 1.763$  for the 3D Ising model and 3D  $Z_2$  lattice gauge theory. The latter follows from the fact that models which are connected by duality transformations have identical values of  $\alpha, \nu$ , since these two exponents can be obtained from scaling of the free energy. On the other hand, certain combinations of the remaining critical exponents, which depend on the degrees of freedom one chooses to describe the transition with, remain invariant. These invariant combinations are given by<sup>48</sup>

$$\frac{\gamma}{2 - \eta}, \quad 2\beta + \gamma, \quad \beta(\delta + 1). \quad (28)$$

The first is a consequence of Fisher's scaling law, the other two follow from Rushbrooke's scaling law. Figure 3 shows the second and third moments for the 3D Ising model for system sizes  $L = 12, 20, 32, 40$  as a function of  $\beta$ , while Fig. 4 shows the corresponding quantities for the 3D  $XY$  model.

#### D. Finite-size scaling of $M_2$ and $M_3$

We first consider the second moments of the 3D  $XY$  model and the 3D Ising model. These exhibit peaks at  $T_c$



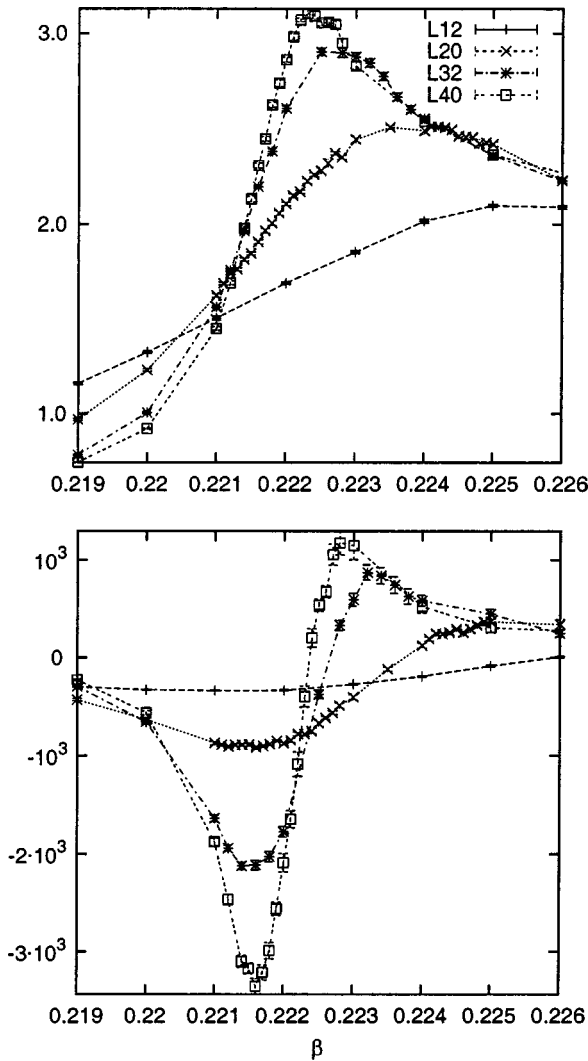


FIG. 3. Second moment (upper panel) and third moment (lower panel) of the action for the 3D Ising model for system sizes  $L = 12, 20, 32, 40$ .

which in principle are amenable to finite size scaling. Figure 5 upper panel shows the finite-size scaling plots of the peaks in the second moment of both models. As is seen from the figure, the peaks grow as  $L$  increases. However, it is clear that none of the scaling plots have reached their asymptotic behavior.

For the 3D  $XY$  model, the apparent scaling for small to intermediate values of  $L$  is clearly spurious, as it levels off for large system sizes. In principle, a *negative* slope should eventually be obtained for asymptotically large system sizes, but the general experience is that impractically large system sizes are required to see this, let alone estimate the slightly negative value of  $\alpha$  with any precision.

For the 3D Ising model, the situation is different in that the peak height grows steadily as  $L$  increases, eventually approaching a straight line on a double-logarithmic plot. Although the quality of the scaling improves with increasing  $L$ , an approximate evaluation of the slope yields  $\alpha/\nu=0.3$  whereas the known value is  $\alpha/\nu=0.175$ . Hence, it is clear

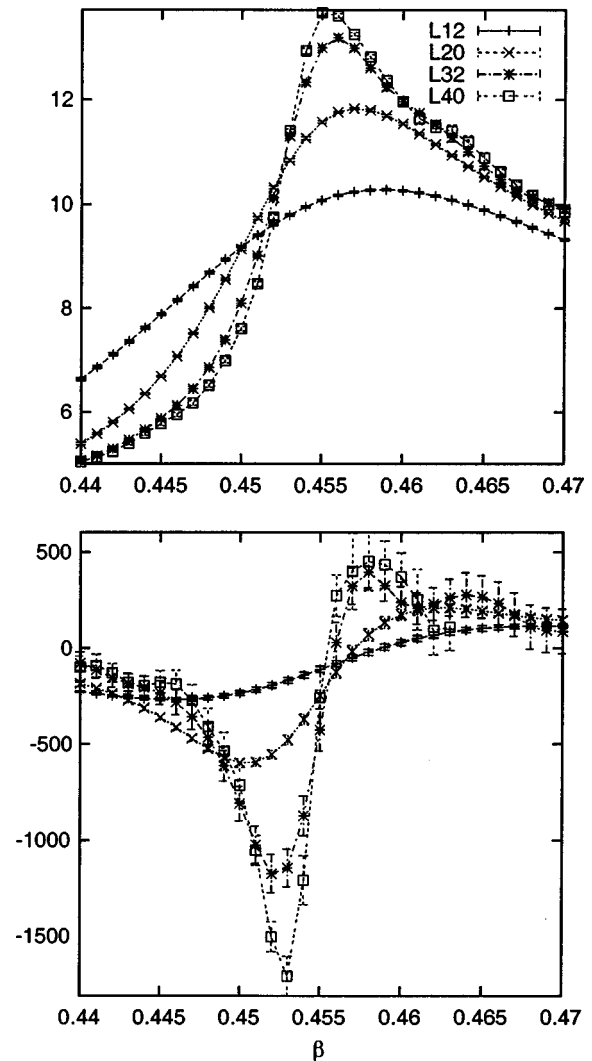


FIG. 4. Second moment (upper panel) and third moment (lower panel) of the action for the 3D  $XY$  model for system sizes  $L = 12, 20, 32, 40$ .

that inaccessibly large systems are required to obtain the specific heat exponent with any accuracy from the second moment scaling analysis.

Consider now the third moment of the action for the 3D  $XY$  and Ising models. The results are given in Fig. 5, middle panel. It is obvious that the quality of the scaling in both cases is vastly improved compared to the results obtained from the second moment. This demonstrates rather convincingly that finite-size scaling of the third moment of the action, i.e., a purely thermodynamic measurement without recourse to order parameters, suffices to bring out that a singular part of the free energy exists in both cases. This would have been difficult to conclude based on the second moment of the action, at least for the 3D  $XY$  model. Note that scaling such as this would not have been found had there not been a nonanalytic part of the free energy. Thus, the quality of the scaling alone suffices to demonstrate the existence of a phase transition. Moreover, the double-peak structure in  $M_3$  permits a separation of  $\alpha$  and  $\nu$  without recourse

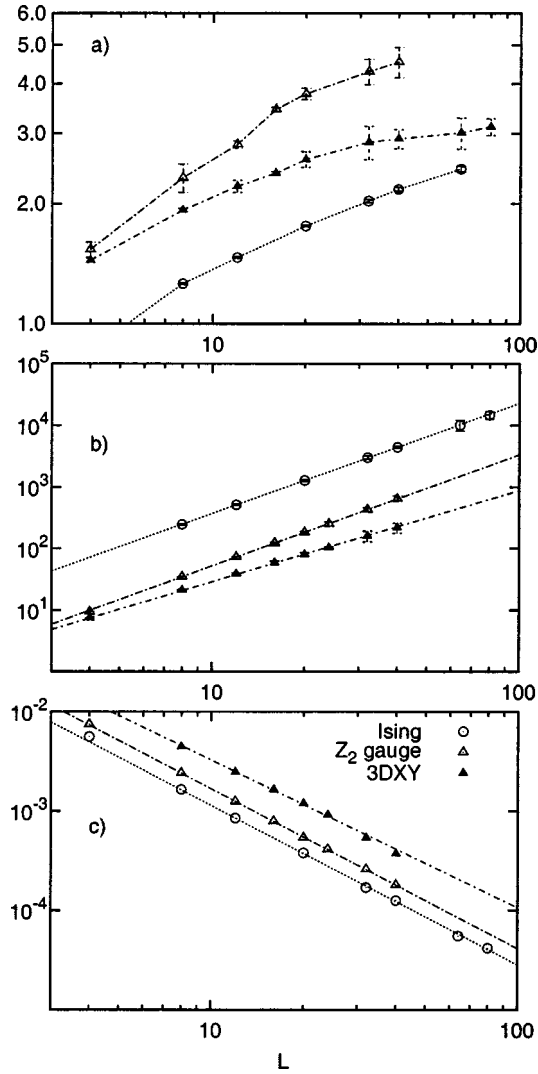


FIG. 5. Finite-size scaling plots for the 3D  $XY$ , 3D Ising, and 3D  $Z_2$  lattice gauge model defined in Eq. (27). (a) The peaks in the second moment of the action demonstrating that very large system sizes are necessary to obtain correct scaling results. For clarity, two of the plots are lowered with a multiplicative factor of 0.7 and 0.45 for the Ising and Ising lattice gauge models, respectively. (b) The peak to peak values of the third moment of the action, demonstrating that correct scaling results are obtained for much smaller system sizes than what is the case for the second moment. Note also the close similarity of the scaling results for the Ising and  $Z_2$  lattice gauge models, which should be identical, up to constants, due to duality. This serves as a quality check on the simulations. (c) The width between peaks in the third moment.

to hyperscaling. The results for the widths between the peaks in the histograms are given in Fig. 5, bottom panel. Note the good quality of the scaling.

The benchmark results for the three models are given in Table I. We see that the error bars of these benchmark values all include the known values of  $\alpha$  and  $\nu$ . Finally, the exponents obtained for the 3D Ising spin model and the 3D Ising gauge theory, are within error bars found to be the same, as they should be from duality of the two theories in three dimensions. Since the degrees of freedom used in the simula-

TABLE I. Critical exponents extracted for the benchmark models, where  $\alpha$  is computed by combining the  $(1 + \alpha)/\nu$  and  $1/\nu$  results.

Model	$(1 + \alpha)/\nu$	$\nu$	$\alpha$
$XY$	$1.46 \pm 0.01$	$0.67 \pm 0.01$	$-0.01 \pm 0.01$
Ising	$1.77 \pm 0.01$	$0.63 \pm 0.01$	$0.11 \pm 0.01$
$Z_2$ gauge	$1.78 \pm 0.02$	$0.63 \pm 0.01$	$0.12 \pm 0.02$

tions are vastly different, this serves as a highly nontrivial quality check on the simulations.

### E. Benchmark simulations of a 3D $XY$ model coupled to a $Z_2$ clock model

To investigate the scaling behavior of the third moment of the action in a well studied 3D theory<sup>49</sup> with two coupling constants and two fixed points of type  $Z_2$  and  $XY$ , we have considered the model

$$Z = \int_{-\pi}^{\pi} \left[ \prod_{j=1}^N \frac{d\theta_j}{2\pi} \right] \exp[\beta H_{XY} + h H_{Z_q}],$$

$$H_{XY} = \sum_{j,\mu} \cos(\nabla_{\mu} \theta_j),$$

$$H_{Z_q} = \sum_j \cos(q\theta_j), \quad (29)$$

defined on a ( $d=3$ )-dimensional cubic lattice with  $N$  sites. The phase  $\theta_j$  resides on every site  $j$  and  $q$  is integer valued.

Let us consider the  $q=2$  theory. By simple inspection of the model we find that the limit  $h \rightarrow \infty$  leads to a twofold symmetry constraint on the phase, and the model becomes exactly the 3D Ising model. The limits  $\beta \rightarrow \infty$  and  $\beta = 0$  are trivial theories. From renormalization group theory, the  $q=2$  model is found to have a  $XY$  phase transition with  $h=0$ , while it exhibits Ising exponents for any other  $h \neq 0$  (at least in the vicinity of  $h=0$ .)

We have performed Monte Carlo simulations on the model Eq. (29),  $q=2$  with system sizes up to  $L=32$ . The resulting exponents from the third moment scaling analysis are given in Fig. 6. We measure  $Z_2$  critical exponents down to very small values of  $h$ . However, it is clear that the critical coupling approaches the 3D  $XY$  value as shown in the upper panel. Note the dramatic increase in both  $(1 + \alpha)/\nu$  and  $1/\nu$  for  $h=0.01$  in the vicinity of the  $XY$  fixed point, where we find that the exponents become even less  $XY$ -like. The value for  $\alpha$  shows a more smooth crossover behavior from 3D  $XY$  value to 3D Ising value as  $h$  is increased from 0. However, the scaling appears not to have reached its asymptotic behavior and the slopes are clearly decreasing for increasing system sizes. We expect this to be due to a cross-over regime in which the cross-over exponent contaminates our estimates, but that all the combinations of exponents eventually will converge towards Ising values, when  $h \neq 0$ .

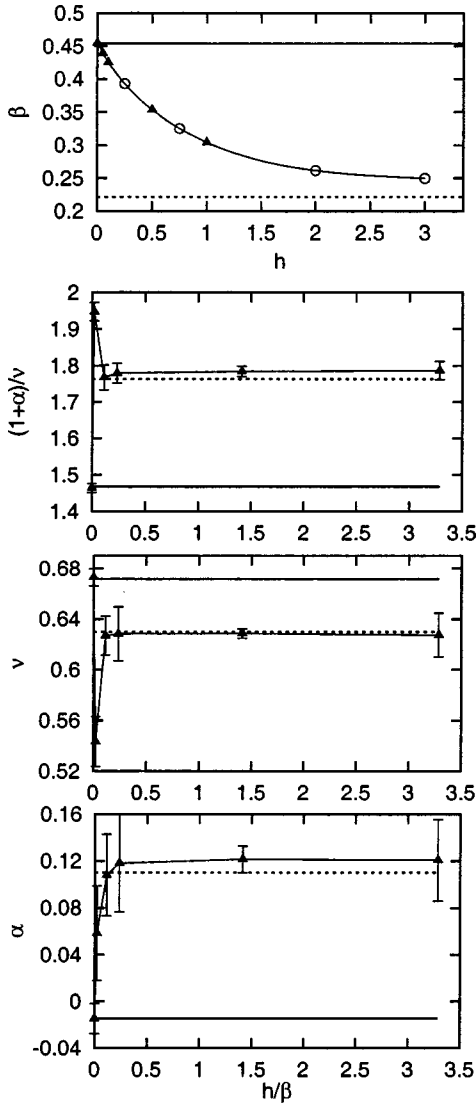


FIG. 6. Upper panel: The phase diagram of the model Eq. (29). The open circles denote points where only the phase transition has been located, while the filled triangles denote points where also the critical exponents have been measured. Lower panels: The three lower panels show the combination of exponents  $(1 + \alpha)/\nu$ , as well as  $\nu$  and  $\alpha$ , as a function of  $h/\beta$ . Note the rapid crossover in  $\alpha$  from the 3D  $XY$  value at  $h=0$  to the 3D Ising value as  $h$  is increased. The dotted and horizontal lines denote 3D  $XY$  and 3D Ising values, respectively, for the various quantities.

#### F. Simulations of the 3D compact Abelian Higgs model $q=2$

We next consider the third moment of the model defined by Eq. (2). The model with  $q=2$  has previously been studied by Monte Carlo simulations on small systems  $L^3$ , with  $L=2,3,4$  many years ago<sup>50</sup> using second moments of the action. A short version of the results to be presented in this section, has already appeared.<sup>19</sup> To our knowledge, no simulations have been performed in  $d=3$  between those presented in Ref. 50 and the much more recent large-scale simulations that have been performed.<sup>19</sup> Due to our observation that scaling of the second moment requires much larger systems than those studied in Ref. 50 in order to obtain reliable

results for exponents, a revisit to the problem seems very appropriate. This is particularly true given the importance the model now has acquired in condensed matter system as a real model for strongly correlated quantum systems at zero temperature in two spatial dimensions.<sup>11,12,2,28</sup> In Ref. 28, precisely such an effective model with  $q=2$  was derived from a proposed microscopic description of charge-fractionalized phases in strongly correlated systems. Specifically, the confined phase of the  $q=2$  model was interpreted as a Mott-Hubbard insulating phase, while the deconfined-Higgs phase was interpreted as a charge-fractionalized insulating phase.

The critical exponents obtained from third moment FSS analysis are presented in Fig. 7. The exponents  $\alpha$ ,  $\nu$ , and the combination  $(1 + \alpha)/\nu$  vary continuously along the critical line showing 3D  $XY$  and  $Z_2$  universality in the  $\kappa \rightarrow \infty$  and  $\beta \rightarrow \infty$  limits, respectively. The  $Z_2$  behavior persists deep into the phase diagram, while we find a broad nonuniversal area in the large- $\kappa$  region. These two areas are joined by a peak in the exponents. To check the dependence of the trajectory, we performed simulations for several slopes at the two extremas, using  $a = \infty$ ,  $a = 1$ ,  $a = -1$  and the direction given by the diagonalization of the fluctuation matrix. Within error bars, all slopes consistently produced the same exponents.

The results appear to rule out that  $Z_2$ - and  $XY$ -critical behaviors are isolated points at the extreme ends of the critical line. However, a feasible suggestion could be that two types of universality,  $Z_2$  and  $XY$ , are separated at a multicritical point on the critical line. We believe this to be ruled out by the strong deviation in  $(1 + \alpha)/\nu$  from  $Z_2$  and  $XY$  values at intermediate  $\kappa/\beta$ . On balance, we thus conclude that the model Eq. (2) defines a fixed-line theory, rather than exhibiting two scaling regimes separated by a multicritical point. However, the  $Z_2$  character of the confinement-deconfinement transition persists to surprisingly large values of  $\kappa/\beta$  on the critical line, see also Fig. 5 of Ref. 50. Fixed-line theories in 2+1 dimensions are known,<sup>51</sup> and nonuniversal exponents imply the existence of marginal operators in Eq. (2), yet to be identified.

#### G. Simulations of the 3D compact Abelian Higgs model $q=3$

The  $Z_q$  spin model and  $q$ -state Potts model are easily seen to be equivalent for  $q=2$  and  $q=3$ .<sup>52</sup> For the  $q$ -state Potts model, it is known that when one generalizes  $q$  to be real-valued, the phase transition in the model in  $d=3$  changes from continuous to discontinuous when  $q$  is increased beyond the value  $q=2.625$ .<sup>53</sup> Hence, both the  $Z_3$  lattice gauge theory and the  $Z_3$  spin model have first order phase transitions. In the limits  $\beta \rightarrow \infty$  and  $\kappa \rightarrow \infty$  the model defined by Eq. (2) reduces to the  $Z_3$ -spin model and 3D  $XY$  model, respectively. If these phase transitions survive on the critical line for finite coupling values, a tricritical point joining the first and second order critical lines is expected to exist. As we shall see, this is precisely what happens.

Therefore, we reach the important conclusion that the model exhibits a first order phase-transition not only for  $\beta = \infty$ , Eq. (7), but also for finite values of  $\beta$ . To identify and investigate the first order phase transitions we have computed histograms of the action (2) at critical coupling con-

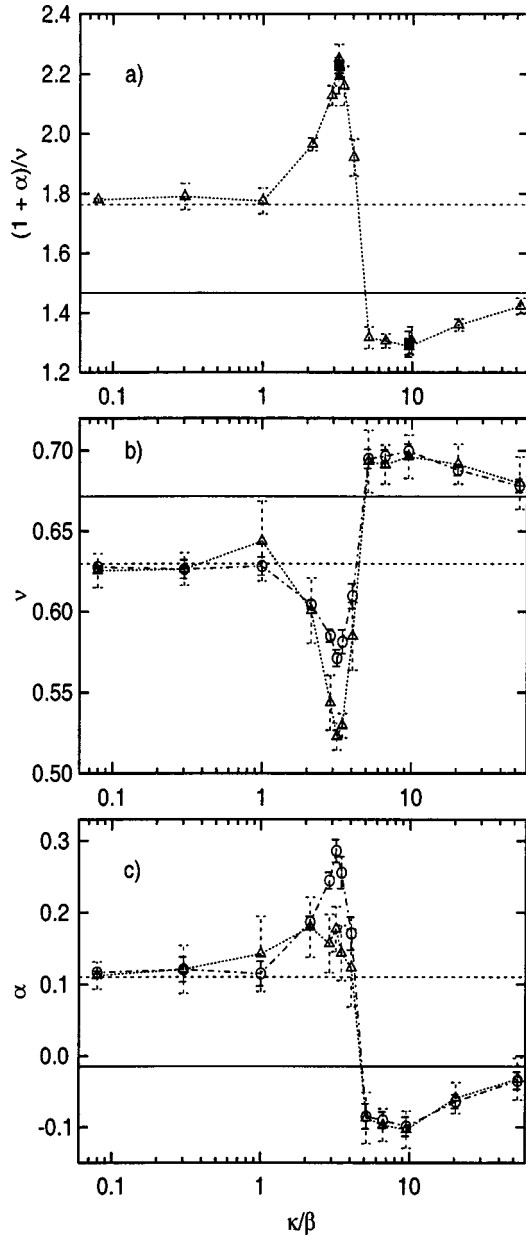


FIG. 7. (a)  $(1 + \alpha)/\nu$  from FSS finite size of  $M_3$  for Eq. (2) for  $q=2$ . Note the variation relative to the  $Z_2$  limit 1.76 (dotted horizontal line) and the  $U(1)$  limit 1.467 (solid horizontal line). (b) Same for the exponent  $\nu$ , computed directly from  $M_3$  ( $\Delta$ ) and combining results for  $(1 + \alpha)/\nu$  with hyperscaling ( $\circ$ ). (c)  $\alpha$  as computed directly from  $M_3$  ( $\Delta$ ) and using results for  $(1 + \alpha)/\nu$  with hyperscaling ( $\circ$ ). The maximum and minimum in (a) have been obtained by crossing the critical line along the trajectory  $\beta(\kappa) = \beta_c + a(\kappa - \kappa_c)$  with  $a = \infty$  ( $\Delta$ ),  $a = 1$  ( $\blacksquare$ ), and  $a = -1$  ( $\blacktriangle$ ) using  $\beta_c = 0.665, \kappa_c = 2.125$  (max.), and  $\beta_c = 0.525, \kappa_c = 5.0$  (min.).

stants. These have a double-peak structure due to the two coexisting phases that characterize a first-order phase transition. The histograms have been produced from large scale Monte Carlo simulations followed by multihistogram reweighting and jackknife error analysis.<sup>42</sup> The results are shown in Fig. 8.

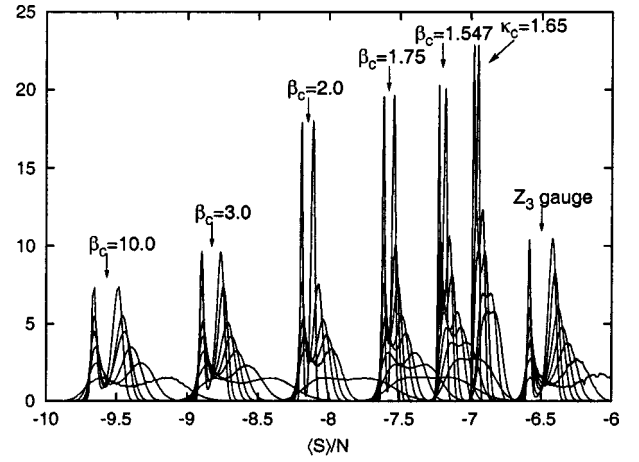


FIG. 8. Normalized histograms of the action (2) for  $q=3$  at the first order phase transition with various critical couplings and system sizes  $L=8,12,16,20,24,32,40,64$ . The histogram height increases with system size. The horizontal axis shows the average value of the action per unit volume, and the histograms have been shifted horizontally for clarity.

A first-order phase transition is characterized by two coexisting phases with the same free energy. There should therefore exist domain walls separating the two phases. The area of the domain walls is related to the energy difference  $\Delta F(L)$  required to keep the two phases separated through the expression

$$\Delta F(L) = \ln P(S, L)_{\max} - \ln P(S, L)_{\min} \sim L^{d-1}, \quad (30)$$

where  $P(S, L)$  is the probability for a value  $S$  of the action in a system of size  $L^d$  and  $L^{d-1}$  is the cross-section area between the ordered and disordered phases.<sup>54</sup> The results shown in Fig. 9 confirm this for system sizes  $L \geq 24$ .

The discontinuity of the action or equivalently the width between the peaks in the histograms is, strictly speaking, not the latent heat. Nonetheless, it can be taken as a reasonably accurate measure of this quantity along a sufficiently small part of the phase transition line. It is important to ascertain whether or not the first-order character of systems persists in the thermodynamic limit. Hence, we plot the discontinuity of the action as a function of system size in Fig. 9, upper panel, and find that the discontinuity of the action is finite at least up to  $\kappa_c = 1.65$ . The first order phase transition becomes increasingly weaker, i.e., the latent heat in the transition is reduced as we approach  $\kappa_c = 1.65$  from below.

Approaching the tricritical point along the first order line, the discontinuity in the action, equivalently the width between the peaks in the histograms, must vanish. From Fig. 9 we have extrapolated the thermodynamic limit of this quantity, and plotted them as a function of the critical coupling in Fig. 10. A linear extrapolation yields an estimate for the tricritical point  $\kappa_{\text{tri}}/\beta_{\text{tri}} = 1.39 \pm 0.06$  corresponding to  $(\beta_{\text{tri}}, \kappa_{\text{tri}}) = (1.23 \pm 0.03, 1.73 \pm 0.03)$ .

On the other side of the tricritical point we have performed a third moment analysis. The exponents are expected

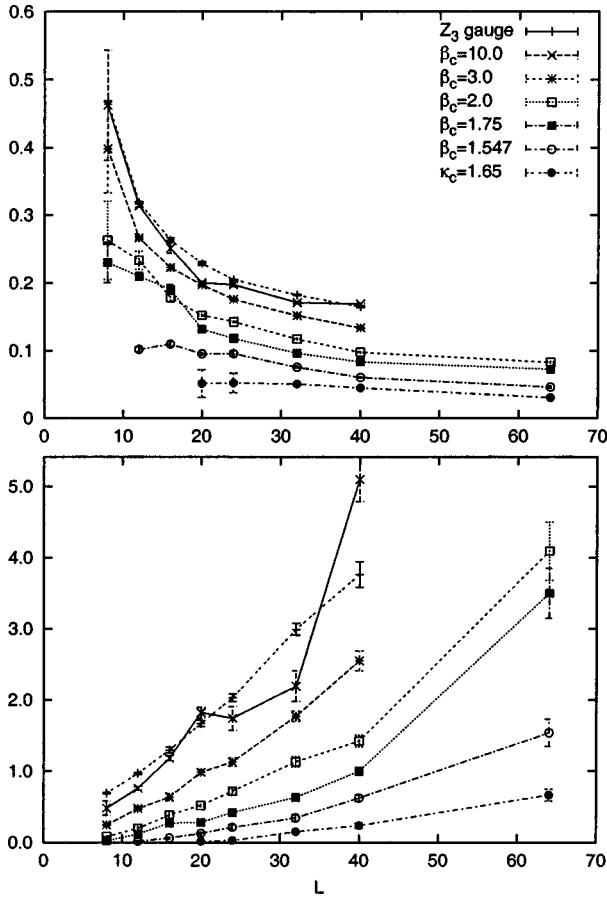


FIG. 9. Upper panel: The discontinuity of the action (2) as a function of system size. Note that the plots seem to be converging towards a finite energy value. Lower panel: The energy difference between the two coexisting phases  $\Delta F(L)$  as a function of system size, same labeling as in the upper panel.

to be those of 3D XY in the large- $\kappa$  limit. Strictly speaking, critical exponents are properties of second order phase transitions. For a first order transition the correlation length stays finite and hence there is no scale-invariance. However, bounds for some of the exponents can be obtained and the

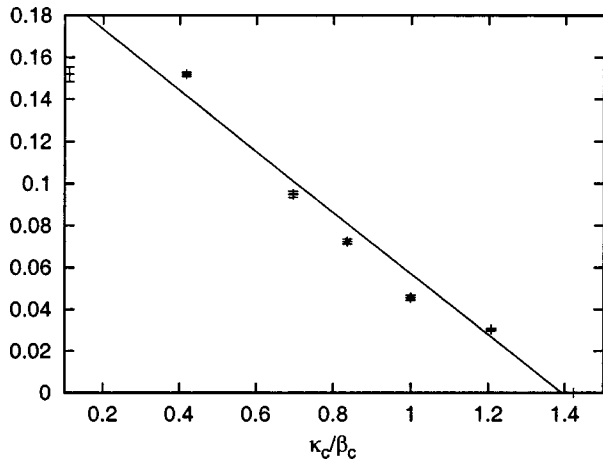


FIG. 10. Width of peaks in histograms as a function of  $\kappa_c/\beta_c$ . The solid line is a linear fit to the data points for  $\kappa_c/\beta_c > 0.8$ .

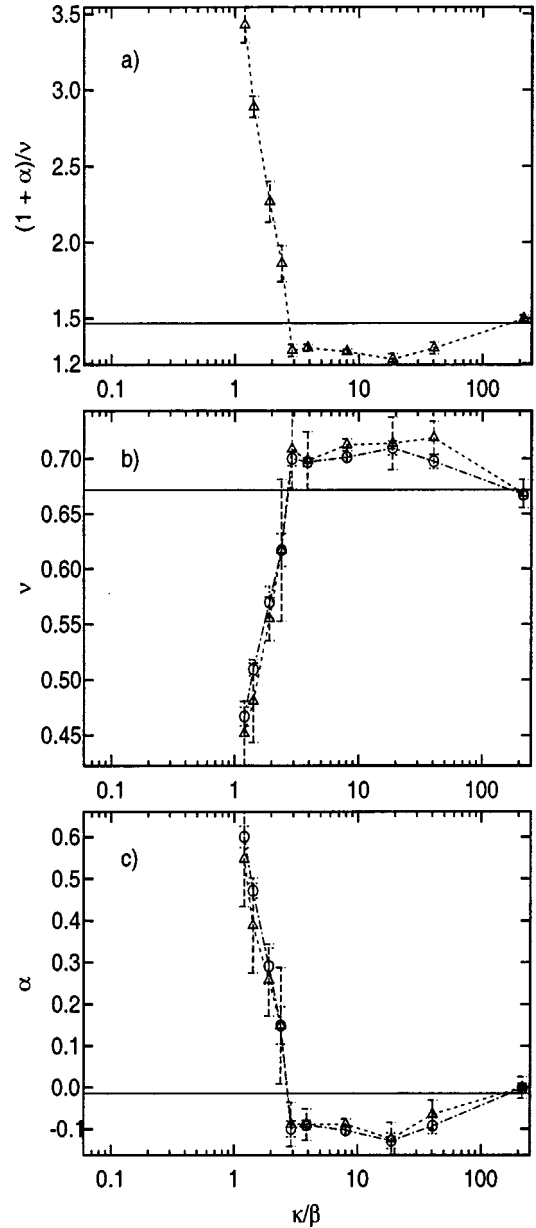


FIG. 11. (a)  $(1 + \alpha)/\nu$  from FSS finite-size of  $M_3$  for Eq. (2) for  $q=3$ . Note the variation relative to the  $U(1)$  limit 1.467 (solid horizontal line) and the violent behavior near the critical point  $\kappa_{tri}$ . (b) Same for the exponent  $\nu$ , computed directly from  $M_3$  ( $\Delta$ ) and combining results for  $(1 + \alpha)/\nu$  with hyperscaling ( $\circ$ ). (c)  $\alpha$  as computed directly from  $M_3$  ( $\Delta$ ) and combining results for  $(1 + \alpha)/\nu$  with hyperscaling ( $\circ$ ).

limits of these bounds correspond to the exponents one would get by relaxing the definitions and formally considering first order transitions.<sup>48</sup> One finds that the limits are  $\alpha = 1$  and  $\nu = 1/d$ , respectively. Hence when approaching the tricritical point we expect  $(1 + \alpha)/\nu = 6$  and  $\nu = 1/3$ .

The critical exponents, given in Fig. 11, agree with the expectations. The exponents are XY-like in the large  $\kappa$  limit while in the region  $2.4 \leq \kappa \leq 50$  the quantity  $(1 + \alpha)/\nu$  is lower than the XY value and hence exhibits nonuniversality similar to what we found for  $q=2$ . At approximately  $\kappa$

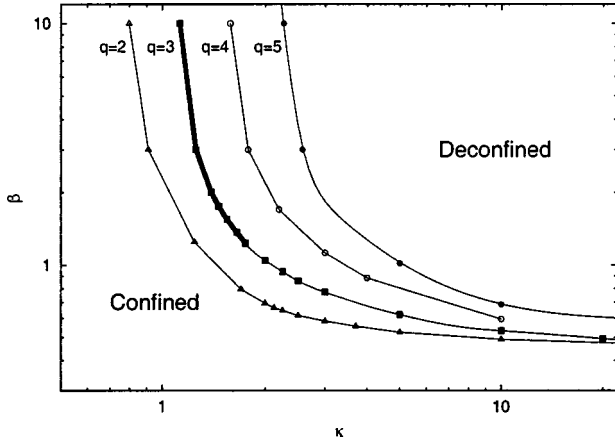


FIG. 12. The phase diagram for the  $d=3$  compact Abelian Higgs model in three dimensions for  $q=2,3,4,5$ . All lines are critical for all values of  $\kappa$  except for the case  $q=3$ , which is first order for  $\kappa < \kappa_{\text{tri}}$  and second order otherwise. The thick solid portion of the  $q=3$  line denotes a first-order transition. Detailed finite-size scaling analysis of the line  $q=2$  shows that the critical exponents  $\alpha$  and  $\nu$  vary continuously along the critical line. This makes the theory defined by Eq. (2) a fixed-line theory with nonuniversal critical exponents, as opposed to a fixed-point theory with universal exponents. The critical line approaches the 3D XY value  $\beta_c = 0.453$  as  $\kappa \rightarrow \infty$  for all values of  $q \in \mathbb{N}$ .

$\sim 2.4$  the exponents rise abruptly towards the first order limiting values. Due to supercritical slowing down, obtaining good quality third moment scaling plots becomes difficult when approaching the tricritical point. Thus, locating the critical point by deciding where the exponents have reached the values one expect in the *limit* of a first order phase transition, is not feasible.

For  $q=3$ , which is a special case in this context (see below), this is very similar to what is now known to happen in the noncompact Abelian Higgs model in  $d=3$ . In that system, a first order phase transition characteristic of type-I superconductivity at small values of the Ginzburg-Landau parameter, is converted to a second order phase transition characteristic of type-II superconductivity. The tricritical value of the Ginzburg-Landau parameter where this change in the character of the phase transition occurs, has recently been determined with precision in large-scale Monte Carlo simulations, to be given by  $0.8/\sqrt{2}$ .<sup>55</sup> This is in remarkable agreement with previous analytical results using duality arguments.<sup>56</sup>

#### H. The phase diagram for $q=2,3,4$

Let us summarize what has been discussed above. The phase structure of the model is given in Fig. 12. From the early Monte Carlo simulations on the model<sup>50</sup> for  $q=2$ , it is known that the critical line  $\beta_c(\kappa)$  approaches  $\lim_{\kappa \rightarrow \infty} \beta_c = 0.454$  while when  $\beta \rightarrow \infty$ , there is a critical value of  $\kappa$  given by  $\kappa_c = 0.761$ . As  $q$  increases, the vertical part of the phase-transition line moves up in  $\kappa$ , while for the values of  $q$  we have considered, the lines are critical except for the case  $q=3$  which is a first order line for large values of  $\beta$ . For any

$q$ , however, we know that the limit  $\kappa \rightarrow \infty$  represents the  $U(1)$  limit, which must exhibit a second order phase transition. Hence, the line for  $q=3$  in Fig. 12 must contain a tricritical point. The first order line for large  $\beta$  terminates at a tricritical point, and is second order for larger values of  $\kappa$ . For  $q=4$ , which is also shown, the phase-transition line is second order. The limit  $\beta \rightarrow \infty$  corresponds to the  $d=3$   $Z_4$  lattice model which is dual to the  $Z_4$  spin model. Using the fact that the symmetry group  $Z_4 = Z_2 \otimes Z_2$ , the universality class of the  $q=4$  phase transition line is expected to interpolate between the Ising case in the limit  $\beta \rightarrow \infty$  and the 3D XY universality class in the limit  $\kappa \rightarrow \infty$ .

Based on what is presented above, we conclude that for  $q \neq 3$ , the model Eq. (2) exhibits a critical line  $\beta_c(\kappa)$  for all values of  $\kappa$ , while for  $q=3$  the phase transition of the model is first order for small values of  $\kappa$  and is converted to a second order phase transition when  $\kappa$  is increased beyond a finite tricritical value.

#### V. CONCLUSIONS

In this paper we have, in addition to a number of benchmark models, considered various lattice gauge models in  $2+1$  Euclidean dimensions, with particular emphasis on the compact Abelian Higgs model with integer gauge charge  $q \geq 2$ . We have seen that for all  $q \geq 2; q \neq 3$ , the phase transition for the model in Eq. (2) is second order such that the entire phase transition line  $\beta_{\text{PT}}(\kappa)$  is critical, i.e.,  $\beta_{\text{PT}}(\kappa) = \beta_c(\kappa)$ . The exponents  $\alpha$  and  $\nu$  which are given by the 3D XY values in the limit  $\kappa \gg \beta$ , and global  $Z_q$  values in the limit  $\beta \gg \kappa$ . For the special case  $q=2$  and for intermediate values of  $\beta$  and  $\kappa$  on the critical line, the exponents vary continuously from the value  $(1+\alpha)/\nu = 1.76$  in the  $Z_2$  limit  $\beta \gg \kappa$  to the value  $(1+\alpha)/\nu = 1.467$  in the  $U(1)$  limit  $\kappa \gg \beta$ . This constitutes a rare example of a *fixed-line* theory with nonuniversal exponents in a three-dimensional system.<sup>51</sup> What the connection to the work of Refs. 14,15 is, where a Kosterlitz-Thouless-like phase transition of unbinding of monopoles in a three-dimensional compact  $U(1)$  gauge theory was found, remains to be investigated. More work is also required to elucidate the special role of  $q=3$  in the compact Abelian Higgs lattice gauge model. Note that this is fundamentally different from what happens in the  $q$ -state Potts model, to which the  $Z_q$  spin model is equivalent only for  $q=2,3$ . In contrast to the compact Abelian Higgs model, the  $q$ -state Potts model has a first order phase transition for all  $q > 2.625$ .<sup>53</sup>

Based on the connection between the model Eq. (2) for  $q=2$  and a recently proposed model of fractionalized phases in strongly correlated systems<sup>28</sup> which is essentially given by Eq. (2), we propose that the universality class of the putative quantum phase transition from a Mott-Hubbard insulator to a charge-fractionalized insulator which the model is supposed to describe, is in the universality class of the  $q=2$  compact Abelian Higgs model characterized by a fixed line of nonuniversal critical exponents varying continuously between the values  $(1+\alpha)/\nu = 1.76$  in the limit  $\beta \rightarrow \infty$ ,  $\kappa$  finite, and  $(1+\alpha)/\nu = 1.467$  in the limit  $\kappa \rightarrow \infty$ ,  $\beta$  finite. However, we

have found that over a significant portion of the critical line of the  $q=2$  compact Abelian Higgs model, the exponents take on values consistent with those of the 3D Ising model. If microscopic models describing such Mott insulator-fractionalized insulator transitions yield the  $q=2$  compact Abelian Higgs model with sufficiently large values of  $\beta$  and small values of  $\kappa$  as an effective theory, then the resulting insulator-insulator transition is in the 3D Ising universality class.<sup>28</sup>

It appears that the study of matter-coupled compact gauge theories would benefit greatly from a precise formulation of a nonlocal order parameter represented by generalized rigidity for such models, as a substitute for the Wilson or Polyakov loops which have proved useful in the pure gauge theories, but which are always perimeter-law bounded in the matter coupled case when the symmetry group of the matter field is a subgroup of the symmetry group for the gauge field.

## ACKNOWLEDGMENTS

A. S. and F.S.N. acknowledge support from the Norwegian Research Council (NFR), Grant No. 148825/432 and from DFG Sonderforschungsbereich 290, respectively. J. S. and E. S. acknowledge NTNU for financial support. A. S. also thanks Professor H. Kleinert and the Institut für Theoretische Physik, Freie Universität Berlin for hospitality. We thank C. Mudry and M. Hasenbusch for useful communications. NFR and the NTNU are acknowledged for support through computing time at the Norwegian High Performance Computing Center (NOTUR). All computations were performed at the Norwegian High Performance Computing Center on an Origin SGI 3800. We particularly thank Dr. K. Rummukainen for providing the software with which we have analyzed our simulation data, and for many useful and enlightening discussions. We also thank Nordita for hospitality.

\*Electronic address: jo.smiseth@phys.ntnu.no

<sup>†</sup>Electronic address: eivind.smorgrav@phys.ntnu.no

<sup>‡</sup>Electronic address: nogueira@physik.fu-berlin.de

<sup>§</sup>Electronic address: joakim.hove@phys.ntnu.no

\*\*Electronic address: asle.sudbo@phys.ntnu.no

<sup>1</sup>See, e.g., C. M. Varma, Z. Nussinov, and W. van Saarloos, Phys. Rep. **360**, 353 (2002).

<sup>2</sup>T. Senthil and M. P. A. Fisher, Phys. Rev. B **62**, 7850 (2000).

<sup>3</sup>S. A. Kivelson, Synth. Met. **125**, 99 (2002).

<sup>4</sup>G. Baskaran, Z. Zou, and P. W. Anderson, Solid State Commun. **63**, 973 (1987); G. Kotliar and J. Liu, Phys. Rev. B **38**, 5142 (1988); G. Baskaran and P. W. Anderson, *ibid.* **37**, 580 (1988); L. B. Ioffe and A. I. Larkin, *ibid.* **39**, 8988 (1989); N. Nagaosa and P. A. Lee, Phys. Rev. Lett. **64**, 2450 (1990); P. A. Lee and N. Nagaosa, Phys. Rev. B **46**, 5621 (1990).

<sup>5</sup>I. Ichinose and T. Matsui, Phys. Rev. B **51**, 11 860 (1995); I. Ichinose, T. Matsui, and M. Onoda, *ibid.* **64**, 104516 (2001).

<sup>6</sup>R. B. Laughlin, in *Proceedings of the Inauguration Conference of the Asia-Pacific Center for Theoretical Physics*, edited by Y. M. Cho, J. B. Hong, and C. N. Yang (World Scientific, Singapore, 1998).

<sup>7</sup>D. H. Lee, Phys. Rev. Lett. **84**, 2694 (2000).

<sup>8</sup>N. Nagaosa and P. A. Lee, Phys. Rev. B **61**, 9166 (2000).

<sup>9</sup>C. Mudry and E. Fradkin, Phys. Rev. B **49**, 5200 (1994); **50**, 11409 (1994).

<sup>10</sup>F. Wegner, J. Math. Phys. **12**, 2259 (1971).

<sup>11</sup>N. Read and S. Sachdev, Phys. Rev. Lett. **66**, 1773 (1991); S. Sachdev and N. Read, Int. J. Mod. Phys. B **5**, 219 (1991).

<sup>12</sup>X.-G. Wen, Phys. Rev. B **44**, 2664 (1991).

<sup>13</sup>Z. Nussinov, J. Zaanen, and A. Sudbó (unpublished).

<sup>14</sup>H. Kleinert, F. S. Nogueira, and A. Sudbó, Phys. Rev. Lett. **88**, 232001 (2002).

<sup>15</sup>H. Kleinert, F. S. Nogueira, and A. Sudbó, hep-th/0209132 (unpublished).

<sup>16</sup>I. F. Herbut and Z. Tešanović, Phys. Rev. Lett. **76**, 4588 (1996).

<sup>17</sup>J. Hove and A. Sudbó, Phys. Rev. Lett. **84**, 3426 (2000).

<sup>18</sup>A. M. Polyakov, Nucl. Phys. B **120**, 429 (1977).

<sup>19</sup>A. Sudbó, E. Smørgrav, J. Smiseth, F. S. Nogueira, and J. Hove, Phys. Rev. Lett. **89**, 226403 (2002).

<sup>20</sup>M. B. Einhorn and R. Savit, Phys. Rev. D **17**, 2583 (1978); **19**, 1198 (1979).

<sup>21</sup>E. Fradkin and S. H. Shenker, Phys. Rev. D **19**, 3682 (1979).

<sup>22</sup>J. Villain, J. Phys. (France) **36**, 581 (1975).

<sup>23</sup>The critical value of  $\beta$  for the isotropic 3D XY/Villain model is very accurately given by  $\beta_c = 1/3$ , see, e.g., A. K. Nguyen and A. Sudbó, Phys. Rev. B **57**, 3123 (1998). The latest and most accurate value reported for the critical coupling that we are aware of, is given by  $\beta_c = 0.333068(7)$ , see T. Neuhaus, A. Rajantie, and K. Rummukainen, *ibid.* **67**, 014525 (2003).

<sup>24</sup>C. Borgs and F. Nill, J. Stat. Phys. **47**, 877 (1987).

<sup>25</sup>M. N. Chernodub, E.-M. Ilgenfritz, and A. Schiller, Phys. Rev. Lett. **88**, 231601 (2002); Phys. Rev. D **67**, 034502 (2003).

<sup>26</sup>M. N. Chernodub, E.-M. Ilgenfritz, and A. Schiller, Phys. Lett. B **547**, 269 (2002).

<sup>27</sup>D. J. Amit, S. Elitzur, E. Rabinovici, and R. Savit, Nucl. Phys. B **210**, 69 (1982).

<sup>28</sup>O. I. Motrunich and T. Senthil, Phys. Rev. Lett. **89**, 277004 (2002); T. Senthil and O. I. Motrunich, Phys. Rev. B **66**, 205104 (2002).

<sup>29</sup>C. Nayak, Phys. Rev. Lett. **85**, 178 (2000).

<sup>30</sup>*Perspectives in Quantum Hall Effects*, edited by S. Das Sarma and A. Pinczuk (Wiley, New York, 1997).

<sup>31</sup>B. Douçot, M. V. Feigel'man, and L. B. Ioffe, Phys. Rev. Lett. **90**, 107003 (2003).

<sup>32</sup>T. Senthil and M. P. A. Fisher, Phys. Rev. Lett. **86**, 292 (2001).

<sup>33</sup>D. A. Bonn, J. C. Wynn, B. W. Gardner, Y.-J. Lin, R. Liang, W. N. Hardy, J. R. Kirtley, and K. A. Moler, Nature (London) **414**, 887 (2001).

<sup>34</sup>I. Affleck, Z. Zou, T. Hsu, and P. W. Anderson, Phys. Rev. B **38**, 745 (1988).

<sup>35</sup>C. Dasgupta and B. I. Halperin, Phys. Rev. Lett. **47**, 1556 (1981).

<sup>36</sup>P. Cea and L. Cosmai, J. High Energy Phys. **11**, 064 (2001).

<sup>37</sup>R. Savit, Rev. Mod. Phys. **52**, 453 (1980). The loop-gas representation of the 3D XY model is  $Z = \sum_{\{Q\}} \sum_{\{J_{j\mu}\}} \delta_{\Delta_\nu J_{j\nu}, 0} \exp(-2\pi^2 \kappa \sum_j J_{j\mu}^2)$ . The 3D XY model is given by the case  $q=0$  in Eq. (2). From Eq. (7) when  $q \rightarrow \infty$ , open-ended vortex configurations are suppressed; the system reverts to the 3D XY model, cf.  $\lim_{q \rightarrow \infty} Z_q = U(1)$ .

- <sup>38</sup>A. Ukawa, P. Windey, and A. H. Guth, *Phys. Rev. D* **21**, 1013 (1980).
- <sup>39</sup>H. Kleinert, *Gauge Fields in Condensed Matter* (World Scientific, Singapore, 1989), Vol. 1.
- <sup>40</sup>Z. Tešanović, *Phys. Rev. B* **59**, 6449 (1999).
- <sup>41</sup>A. K. Nguyen and A. Sudbø, *Phys. Rev. B* **60**, 15 307 (1999); *Europhys. Lett.* **46**, 780 (1999).
- <sup>42</sup>J. Hove, S. Mo, and A. Sudbø, *Phys. Rev. Lett.* **85**, 2368 (2000).
- <sup>43</sup>Note that this contrasts with the results of Ref. 44, where the  $U(1)$  symmetry group of the matter field is not contained in the  $Z_2$  symmetry group of the gauge field. Hence, the results of Ref. 13 are not relevant. In Ref. 44, the Polyakov loop could therefore be used with success to map out the phase-structure of the theory, even if the gauge theory considered in Ref. 44 is matter coupled.
- <sup>44</sup>R. D. Sedgewick, D. J. Scalapino, and R. L. Sugar, *Phys. Rev. B* **65**, 054508 (2002).
- <sup>45</sup>See, for instance, J. Cardy, *Scaling and Renormalization in Statistical Physics* (Cambridge University Press, Cambridge, 1996).
- <sup>46</sup>A. D. Bruce and N. B. Wilding, *Phys. Rev. Lett.* **68**, 193 (1992); J. L. Alonso *et al.*, *Nucl. Phys. B* **405**, 574 (1993).
- <sup>47</sup>R. J. Baxter, *Exactly Solved Models in Statistical Mechanics* (Academic Press, London, 1982), Chap. 10. The generalized Ising model formulation of the 8-vertex square lattice model is also given in, e.g., F. Y. Wu, *Phys. Rev. B* **4**, 2314 (1971); L. P. Kadanoff and F. Wegner, *ibid.* **4**, 3989 (1971). Another planar model exhibiting power-law singularities in the specific heat with nonuniversal exponents, is the square lattice Ashkin-Teller model, which also features a four-spin coupling.
- <sup>48</sup>J. Hove, Ph.D. thesis, Norwegian University of Science and Technology, 2002.
- <sup>49</sup>D. R. Nelson and R. A. Pelcovits, *Phys. Rev. B* **16**, 2191 (1977).
- <sup>50</sup>G. Bhanot and B. A. Freedman, *Nucl. Phys. B* **190**, 357 (1981).
- <sup>51</sup>The three-dimensional noncompact  $U(1)$  gauge theory with Chern-Simons term added, is another example of a fixed-line theory with nonuniversal exponents. However, in this case both parity and time-reversal symmetry are broken. See, for instance, W. Chen, M. P. A. Fisher, and Y.-S. Wu, *Phys. Rev. B* **48**, 13 749 (1993); C. de Calan, A. P. C. Malbouisson, F. S. Nogueira, and N. F. Svaiter, *ibid.* **59**, 554 (1999); H. Kleinert and F. S. Nogueira, *J. Phys. Stud.* **5**, 327 (2001).
- <sup>52</sup>This is easily seen from the Hamiltonian for the  $Z_3$  model  $H = -J\sum_{\langle i,j \rangle} \cos[(2\pi/q)(s_i - s_j)]$ , with  $s_i - s_j = 0, 1, 2$ . When  $s_i - s_j = 0$ , the cosine term is 1, otherwise it is  $-1/2$ . Thus, we may also write  $H = -J\sum_{\langle i,j \rangle} [1 + \delta_{s_i, s_j}]/2$ , which is, up to constants, the Hamiltonian for the three-state Potts model. This correspondence is special for  $q=3$  (and  $q=2$ ), since only in these two cases does the  $Z_q$  spin model have a Hamiltonian with only two values on each link connecting nearest neighbor points on the lattice, which is the basic property of the  $q$ -state Potts model (for all values of  $q$ ).
- <sup>53</sup>F. Gliozzi, *Phys. Rev. E* **66**, 016115 (2002).
- <sup>54</sup>J. Lee and J. M. Kosterlitz, *Phys. Rev. Lett.* **65**, 137 (1990).
- <sup>55</sup>S. Mo, J. Hove, and A. Sudbø, *Phys. Rev. B* **65**, 104501 (2002).
- <sup>56</sup>H. Kleinert, *Lett. Nuovo Cimento* **35**, 405 (1982).